Separation of Seyferts and LINER Galaxies Using Eddington Ratio Derived from the Spectral Energy Distribution

Spencer L. Kirn
Physics Department, The College of Wooster, Wooster OH 44691 USA
(Dated: May 6, 2015)

In this study the Eddington Ratio of an AGN was examined to see how it would effect the the placement of a galaxy on a BPT diagram. The Eddington Ratio of an object is the ratio of the total light output of that object to the maximum amount of light it can emit based on the mass of the object. BPT diagrams are diagrams that utilize emission line ratios in order to classify galaxies as star forming, Seyfert, or LINER. Seyfert and LINER galaxies are two different types of active galaxies, where Seyfert have spectra with emission lines from very highly ionized atoms and LINERs have spectra with emission lines from low ionized atoms. It was theorized that LINERs would have a lower Eddington Ratio leading to a trend in the placement on a BPT diagram as Seyferts transition to LINERs. LINERs were believed to have a lower Eddington Ratio because while they can be the same size as a Seyfert, they have emission lines from lower ionized atoms. This led to the belief that the photons coming from the nuclei of the LINER were less energetic. The Eddington Ratio was found by analyzing the spectral energy distribution (SED) of 12 galaxies. A SED is a plot of the luminosity of light at every frequency. To find the total amount of light from this plot the area under the curve was found using an integral. This area was divided by the Eddington Limit of the galaxy and thus the Eddington Ratio was created. No correlation was found between the Eddington Ratio and the placement on a BPT diagram.

I. INTRODUCTION

Seyfert galaxies were first observed by Carl Seyfert in 1943. He noticed several galaxies with strong broad emission lines especially hydrogen, whose lines were sometimes broader than all of the other lines. Since these galaxies were observed many other similar galaxies have been observed with slightly different traits. Some examples of these are Seyferts, Quasars, BL Lac Objects, and LINERS. All of these astronomical objects can be classified into one class of galaxy called Active Galactic Nuclei or AGN [1]. For this project I focused specifically on Seyfert and LINER galaxies. The research performed here is an extension of Stern and Laor's [2][3] 2012-2013 set of papers studying type 1 AGN at low redshift. Specifically I wanted to analyze data from Seyfert and LINER galaxies to see how their Eddington ratio would affect their placement on a BPT diagram and to see if there could be further separation between Seyfert and LINER galaxies based on the Eddington ratio. I believed that LINERs would tend to have a lower Eddington Ratio based on their definition. Eddington Ratios and BPT diagrams are both discussed further in section II.

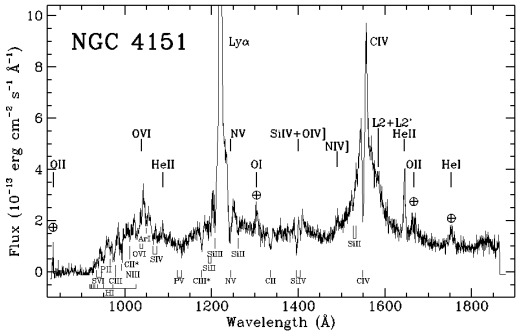

FIG. 1: Spectrum for NGC 4151, a type 1 Seyfert Galaxy. In this spectrum you can see very strong emission lines coming from highly ionized elements. These emission lines are what tell us this is a type 1 Seyfert galaxy. This image was borrowed from source [4]

A. Seyfert Galaxies

Seyfert galaxies are defined as lower luminosity Active Galactic Nuclei. Originally they were defined as spiral galaxies that appeared to have a star superimposed onto the center of the galaxy. Now the definition has grown to define galaxies that have very strong high-ionization emission lines in their spectrum mostly coming from an extremely bright nucleus, hence the name Active Galactic Nuclei. An example of theses spectra can be seen in Fig. 1. In this figure the peaks seen all correspond to highly ionized atoms such as, [FeVII] and [NeV]. Here the notation [FeVII] means six times ionized iron, therefore [NeV] refers to four times ionized nitrogen. This is four times ionized nitrogen because [NeI] would refer to nonionized nitrogen. The spectra in Fig. 1 is representative of type 1 Seyfert galaxies. There are also type 2 Seyfert galaxies whose spectra differ based on the narrow lines that appear that do not in type 1 spectra. Type 2 Seyferts, however, are not relevant to the work done for this paper.

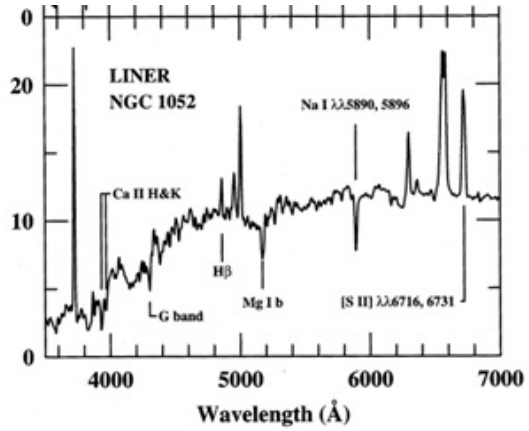

FIG. 2: Emission line spectra NGC 1052, a typical LINER galaxy. Compared to Fig. 1 this is a similar spectra except the emission lines originate from much lower ionized atoms. This image was borrowed from source [5].

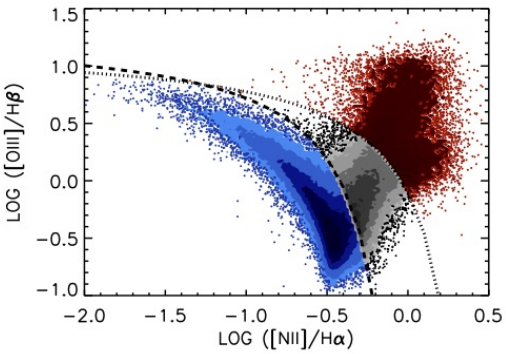

FIG. 3: log[OIII]/Hβ vs. log[NII]/Hα BPT diagram. The two curved lines on the diagram separate AGN and star forming galaxies. The blue colored data points below and to the left of the dashed lines represent star forming galaxies, while the red colored data points above and to the right of the dotted line represent AGN. The grey data points between the dotted and dashed lines represent "composite" galaxies, or galaxies that have characteristics of both AGN and star forming galaxies. This figure was borrowed from source [7].

B. LINER Galaxies

Low-Ionization Nuclear Emission-Line Regions, or LINERs, were first observed by Heckman in 1980. The spectra of these galaxies closely resemble the spectra of Seyfert 2 galaxies, except the low-ionization emission lines, such as [OI], non-ionized oxygen, are very strong instead of the very highly ionized atoms seen in Seyferts. Because they have low-ionization lines there must not be as many photons with high enough energy to knock out electrons from already ionized atoms. This led to the theory that LINERs would have a lower Eddington Ratio than Seyferts because they had less energetic photons. A typical spectrum for a LINER galaxy can be seen in Fig. 2, which represents the spectrum for NGC 1052[1].

II. THEORY

A. BPT Diagrams

A BPT diagram is an emission line ratio graph that is used to separate star-forming galaxies and AGN. These graphs were first created in 1981 by Baldwin, Phillips, and Terlevich and were thus named BPT after the three founders. In their paper they wanted to find a way to definitively separate many of the galactic objects that had been defined by their different spectra. To accomplish this they decided to use emission line ratios. Through their study they found if the ratio of the strength of the [OIII](λ=5007Å) emission line and the Hβ(λ =4861Å) emission line is plotted against the ratio of the strength of the [NII](λ=6584Å) and the Hα(λ=6563Å) on a log-log plot you could separate the star forming galaxies from the AGN [6]. Fig. 3 represents a log([OIII]/Hβ) vs. log([NII]/Hα) BPT diagram. In this graph we can see two different curved lines. The red dots above and to the right of the dotted line represent AGN, while the blue dots below and to the left to the dashed line represent star forming galaxies. The grey dots in the middle represent galaxies that have characteristics of both AGN and star forming galaxies and are referred to as composite galaxies [7].

The [NII]/Hα is not the only ratio used to plot along with [OIII]/Hβ. The two other emission line ratios commonly used are [SII]/Hα and [OI]/Hα, both of which are plotted as the x-axis on separate diagrams with [OIII]/Hβ as the y-axis for both. Fig. 4 shows the difference between the three diagrams. In each diagram there is a curved line, this line is the line that divides the star forming galaxies and the AGN just as in Fig. 3. The reason the [SII] and [OI] graphs were focused on in this study was because in these graphs the LINER and Seyfert galaxies are also able to be separated. In the SII and OI graphs seen in Fig. 4 there is a straight dotted line coming out of the main curve. This line represents the separation point for LINER and Seyfert galaxies. In both graphs below the line are LINER galaxies and above it are Seyfert galaxies. Although what is defined as a LINER in one graph is not always a LINER in the other, these galaxies usually sit near the dividing line in both graphs. In their paper Kewley et al. [9] found the equations for these lines. They found that the curve separating star forming galaxies and AGN to be

$$\log\left(\frac{[\mathrm{OIII}]}{\mathrm{H}\beta}\right) = \frac{0.61}{\log\left(\frac{[\mathrm{NII}]}{\mathrm{H}\alpha}\right) - 0.05} + 1.3 \qquad (1)$$

$$\log\left(\frac{[\mathrm{OIII}]}{\mathrm{H}\beta}\right) = \frac{0.72}{\log\left(\frac{[\mathrm{SII}]}{\mathrm{H}\alpha}\right) - 0.32} + 1.3 \qquad (2)$$

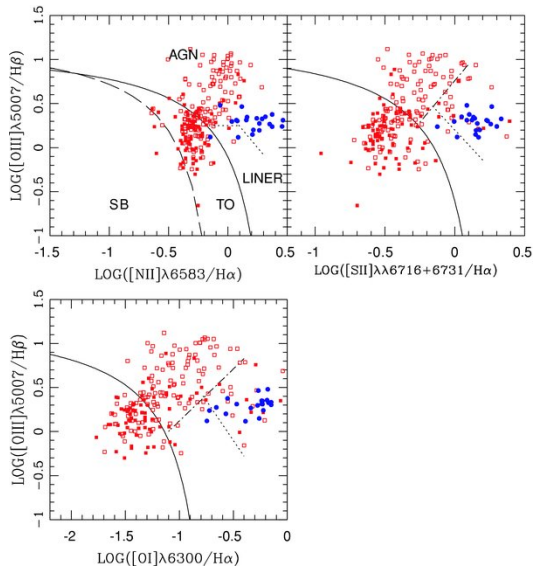

FIG. 4: Image showing the differences between the three main kinds of BPT diagrams. All diagrams have a curve dividing the star forming galaxies and the AGN. In the SII and OI graphs, the top right and bottom graphs respectively, however, there is a way to divide the Seyfert and LINER galaxies. This is why these graphs were focused on for this study. Picture borrowed from [8]

$$\log\left(\frac{[\mathrm{OIII}]}{\mathrm{H}\beta}\right) = \frac{0.73}{\log\left(\frac{[\mathrm{OI}]}{\mathrm{H}\alpha}\right) + 0.59} + 1.33 \tag{3}$$

where the emission line ratio in the denominator refers to the emission line ratio on the x-axis of the graph. Any galaxy that falls below these lines are considered star forming, while any galaxy above these lines would be an AGN. They also found the the equation for the line dividing LINER and Seyferts in the [OI] and [SII] graphs to be

$$\log\left(\frac{[\mathrm{OIII}]}{\mathrm{H}\beta}\right) = 1.89\log\left(\frac{[\mathrm{SII}]}{\mathrm{H}\alpha}\right) + 0.76 \tag{4}$$

$$\log\left(\frac{[\mathrm{OIII}]}{\mathrm{H}\beta}\right) = 1.18\log\left(\frac{[\mathrm{OI}]}{\mathrm{H}\alpha}\right) + 1.30 \tag{5}$$

where again the emission lines ratios on the right side of the equation represent the emission line ratio represented on the x-axis [9]. Any AGN that was above these lines would be a Seyfert, while any galaxy below these would be a LINER. Using these equations we will be able to create and manipulate our own BPT diagrams. These equations would be used to rotate the standard BPT diagram such that the Seyfert/LINER division line would be the y-axis. This allowed for easier analysis of the how the Eddington ratio affects the placement of these galaxies in relation to the dividing line.

B. Eddington Limit

The Eddington limit for stellar objects is defined as the limit for stability against radiation pressure. If a star is more luminous than this pressure it will push out its outer layers in order to reach this stability point. The equation for this limit

$$L_{EDD} = \frac{4\pi c G M m_H}{\sigma_T}, \tag{6}$$

where G is the universal gravitational constant, m_H is the mass of Hydrogen, and σ_T is the Thompson scattering cross-section [10]. This limit is not just valid for stars, however, the Eddington limit is useful for any spherical source powered by accretion, such as an active galactic nuclei.

For AGN, the Eddington luminosity is seen as the maximum luminosity for an object of mass M powered by spherical accretion. To find the Eddington Limit of an AGN we can still use Eqn. 6 [1]. However we can adjust this equation to have M_{BH} in solar masses

$$L_{EDD} = 1.38 \times 10^{38} \frac{\mathrm{erg}}{\mathrm{s}} \times \frac{M_{\mathrm{BH}}}{M_\odot} \tag{7}$$

where the constant in the front of the equation comes from combining all of the constants in Eqn. 6 and $M_\odot$ is 1 solar mass. We will use this limit to create the Eddington Ratio, L/L_{EDD}, which tells us the percent of the total possible luminosity the AGN is creating. In order to find M_{BH}, the mass of the black hole we can use the equation derived by Stern and Laor, Eqn. 2 in source [2]

$$\log\frac{M_{\mathrm{BH}}}{M_\odot} = 7.4 + 2.06\log\Delta v_{1000} + 0.545\log L_{bH\alpha,44} \tag{8}$$

where Δv_{1000} is the width of the broad Hα line divided by 1000 and $L_{bH\alpha,44}$ is the luminosity of the broad Hα line divided by 44. With the limit on the total luminosity the only other value that needs to be found is the total luminosity, which can be found using the spectral energy distribution of the galaxy.

C. Spectral Energy Distribution

In their paper Stern and Laor[2][3] cited an equation derived by Greene & Ho [11] based on the same two variables as Eqn. 8 to find the Eddington ratio

$$\log\frac{L}{L_{EDD}} = 0.6 - 2.06\log\Delta v_{1000} + 0.455\log L_{bH\alpha,44}. \tag{9}$$

Eqn. 9 was necessary in their case because they were using an extremely large sample size, 3077 objects, and not all of the objects in their sample had data in enough light bands to create a full spectral energy distribution (SED).

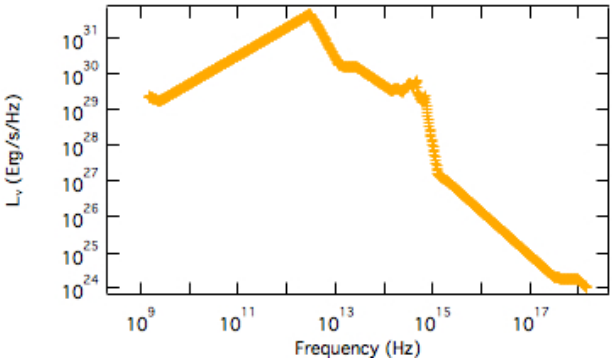

FIG. 5: Spectral energy distribution of NGC 4619 a LINER galaxy. These graphs utilize logarithmic scales to show the relation between the luminosity and the frequency. The graph is composed of straight lines connecting points. This is because we do not have at data on every infinitesimal frequency interval, instead we have data for the luminosity in different bands, such as the J, H, and K bands in the IR. By plotting these and connecting them we can get a good estimate on what the total luminosity of the star is. For this star the total luminosity is 4.83×10^{44} erg/s based on the SED.

A SED is a plot used to show the intensity of light at each frequency. In order to create a full SED there must be sufficient data from X-ray to infrared energies. An example SED compiled in this study can be seen in Fig. 5, this is the SED for NGC 4619 a LINER galaxy. In this diagram it can be seen that there is not a continuous curve of light energy at every frequency as one would expect. This is simply because it is not practical to be able to get a measurement of the luminosity at every infinitesimal frequency throughout the spectrum. Instead the luminosity of the light in a certain region of the spectrum is found and plotted as one single point. For example in the infrared there are three different bands of light; J, H, and K_s. These correspond to 250 THz, 176 THz, and 136 THz respectively. By finding the luminosity in each of these bands then connecting them with a line we get a good estimate of what the curve looks like. This can be seen in Fig. 5 where there are straight lines that end in a sharp turn in the graph. These occur because there is a data point at that local peak and from there it will turn and go to the next data point. Obviously this is not an exact method and it will not give us the exact luminosity, but it gives a good estimate. It is a good estimate because if there is a drop from one point to another, then one would assume that the light in between the two points would gradually become less luminous, we would not expect a sharp drop from one wavelength to the next next integer wavelength. The total luminosity of the galaxy is approximated by integrating the SED to find the total area under the curve. This gives us the total luminosity in all of the light bands, which is equivalent to the total luminosity. This total luminosity can then be divided by the Eddington luminosity to find the percent of luminosity possible the AGN is emitting.

TABLE I: Sample of Data Used

Name	LogLHa	LogLHb	LogLSII	LogLOI	LogLOIII
NGC 3884	40.3	39.8	40.6	40	40.1
NGC 4619	39.5	39	39.8	39.3	39.9
UGC 06614	40.1	39.5	40	39.9	40

III. DATA COLLECTION

The data sample used by Stern and Laor[2][3] in their papers was the starting point for the data set used in this study. For the purposes of this study the full 3077 galaxies were not needed nor was it possible to analyze all 3077. The first galaxies that were eliminated from the sample were any star forming or composite galaxy. This cut 1002 galaxies. Galaxies with measurements in a wide range of light bands were necessary. For this reason any galaxy that did not have measurements in all bands from the infrared to the X-ray were tossed out of the sample. This process cut the sample down from 3077 galaxies to 737 galaxies. Of this 13 galaxies were LINERs in both the [SII] and the [OI] graphs, 7 were LINERs in the [SII] but Seyferts in the [OI], 18 were LINERs in the [OI] but Seyferts in the [SII], the rest of the 699 galaxies were Seyferts. All of the galaxies in the sample now had data in all reported light bands, but it was still too large. To deal with this the galaxies were filtered by redshift and Seyfert galaxy with a redshift higher than z=0.05 were cut. This restriction could not be placed on the LINERs as there were far fewer of them thus all the LINERs were kept. This brought the sample size down to 127 galaxies, all of which had data in all light bands and also had a very low redshift. With this sample 12 galaxies spanning different BPT definitions; LINER in [OI] and [SII], Seyfert in both, and Seyfert in one and LINER in one, were analyzed individually based on their SED. Because they were analyzed individually it was not possible to to analyze the entire sample. An example of the data reported in the sample is seen in table 1. This is only showing a part of the full data shown for each galaxy. In this table logLHa is the logarithm of the luminosity of the Hα line, LogLHb is the the same thing for the Hβ line, then for the logarithm of the intensity of the [SII], [OI], [OIII] lines for the last three columns respectively. The three galaxies in the table are galaxies that were analyzed by their SEDs, the first two are defined as LINERs in both [SII] and [OI] while the last one is a galaxy that is defined as a LINER in [OI], but a Seyfert in [SII].

IV. RESULTS AND ANALYSIS

Before analyzing the SEDs, BPT diagrams were made of the full 127 galaxy sample. An example of one of these graphs can be seen in Fig. 6. The quantization of the data points comes simply because the data was

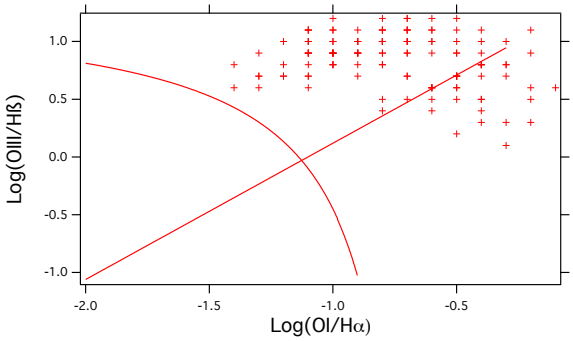

FIG. 6: BPT diagram made using all of the 127 galaxies in the final data set. It can be seen in this graph that the data actually looks quantized. This is simply because the data for the intensity was reported as a logarithm and was only carried to three significant figures. This means that, when finding Log([OIII]/Hβ), for example, the points had to be subtracted, which only allowed for certain values. In reality this graph would look more like the graphs in Fig. 4. The two lines in the graph are the lines derived by Kewley et al. [9]

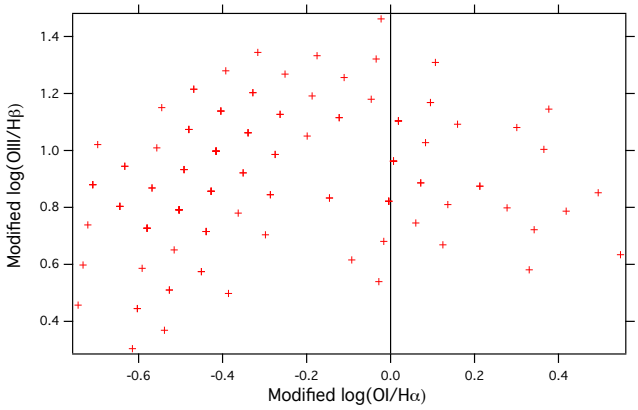

FIG. 7: Graph of the shifted and rotated BPT diagram. The vertical line is the y-axis, which represents the divide between Seyferts and LINERs. LINERs on the positive side of the y-axis and Seyferts on the negative.

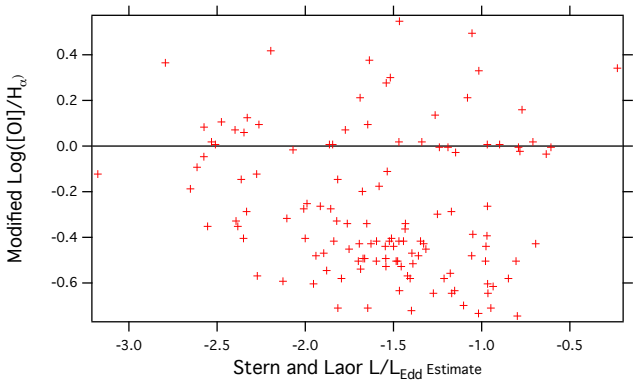

FIG. 8: Plot of the x-axis from Fig. 7 (Modified Log([OI]/Hα)) vs. L/L_{EDD}. Seyfert galaxies are below the x-axis and LINERs above it. A very slight trend with the Seyfert galaxies can be seen as the Eddington ratio increases the modified [OI] ratio increases, but there are enough outliers that this is even a stretch. There is not any noticeable trend with the LINER galaxies.

reported as the logarithm of the intensity of the emission lines. This meant that to find the ratio the data points actually needed to be subtracted due to the rules of logarithms. This only allowed for a limited number of values for the ratio, typically just one significant figure. An example of this can be seen with NGC 3884 in Table 1. The Log([OIII]/Hβ) ratio is found by subtracting LogLHb from LogLOIII to get 0.3. This graph would really look like those in Figs. 3 and 4.

The point of this graph was to find the intersection of the two Kewley lines. This intersection was needed so that the graph could be rotated such that the dividing line between LINERs and Seyferts was the y-axis. Having this line be the y-axis allowed us to plot the rotated x-axis, where the zero point is the line, against the Eddington ratios to see if there is a trend. This intersection was found to be $(-1.13 \pm 0.003, -0.031 \pm 0.003)$. Using this and the angle of the straight line dividing LINER and Seyfert, $\theta_{OI} = 0.703$ Rad. The rotation was done using a simple rotation matrix, which resulted in the following equations

$$x' = x\cos(\theta) - y\sin(\theta) \tag{10}$$

$$y' = y\cos(\theta) + x\sin(\theta) \tag{11}$$

where the [OIII] ratio was the y axis and the [SII] and the [OI] ratios were the x-axes in their respective graphs. The angle used for the [SII] graph was $\theta_{SII} = 0.4867$ Rad and the coordinate for the intersection in the [SII] graph was $(-0.317 \pm 0.008, 0.16 \pm 0.015)$.

With these rotated graphs in hand the L/L_{EDD} estimate from Eqn. 9 was plotted to see if any kind of trend could be spotted. Fig. 8 is an example of these plots. No trend can be seen with these. One might say there is a slight trend with the Seyfert galaxies, as their Eddington ratio decreases the move towards the LINERs, but it is a very weak trend as there are many outliers. There is no noticeable trend whatsoever for the LINERs because they are totally spread out. The [SII] graph was very similar to this one, but with even less of a trend with the Seyferts. There was no way to even differentiate the Seyferts and the LINERs in the [OIII] graphs.

The estimate derived by Stern and Laor for the Eddington ratio gave no trends, but the equation used to find the Eddington ratio relies on the assumption that strength of the broad Hα line and the width of it give a good estimate of the total luminosity of the object. Another way to find the total luminosity of an object is to find the SED and integrating to find the total area under the curve. To find the SED the program IRIS, created by the US Virtual Astronomical Observatory, was

used[12]. This program was able to pull data from the NASA/IPAC Extragalactic Database (NED) and compile that data into a graph that showed the full SED as seen in Fig. 5. This figure shows the data from IRIS that had been imported into Igor Pro.

Each galaxy was studied individually using SED analysis instead of in large sets. This being the case a manageable amount of galaxies needed to be selected. Due to time restrictions only 12 galaxies were selected to be analyzed further. Four galaxies defined as LINERs in both [OI] and [SII] diagrams, four galaxies defined as Seyferts in both, and two galaxies defined as LINERs in just [OI] and two galaxies defined as LINERs just in [SII] were selected in order to give as wide of a range as possible. The specific galaxies were chosen based on the amount of available data on NED.

Once the galaxies were selected their data was loaded into IRIS individually and the redshift was adjusted. As NED has a huge amount of data from many different surveys the data had to be edited down such that there was just one data point in each band. When there were several data points for one frequency the point selected was based on the smallest lens aperture and based on the fit model for the SDSS observed data in the visual. The SDSS model chosen was MODEL. The selections were kept consistent through all AGN studied.

As soon as the data were selected they were put onto a graph and using the interpolate function in Iris the data points were connected. From here the interpolated SED was loaded into Igor as flux density (Jy) vs. frequency (Hz). In order to analyze the SED the flux density had to be converted from Jansky (Jy) to Erg/s/cm^2/Hz to keep consistent units. Using

$$L_\nu = F_\nu 4\pi d^2 \tag{12}$$

the flux density was converted to the luminosity density where d is the distance of the galaxy from Earth in cm. Once calculated L_ν comes out with Erg/s/Hz. With this the total luminosity of the galaxy can be found. Although for the purpose of the Eddington Ratio the total luminosity of the entire galaxy is unnecessary, what is really needed is the luminosity of the nucleus of the galaxy. To find this the luminosity of the host galaxy needs to be subtracted from the total luminosity.

There is no way to find the exact luminosity of the host galaxy, so we found a standard inactive galaxy, NGC 221, and used its SED as a template for the host galaxy. A standard inactive galaxy can model the host galaxy as it has a dark nucleus thus all of the light emitted from is coming from the stars that make up the system. This was done by scaling the SED of the inactive galaxy to the SED of the AGN. It was scaled by finding a point in the near IR, around 10^{14} Hz[13], and matching it to that point in the SED of the AGN. The AGN SED is matched here because this is the highest point in the inactive galaxy's SED and it can be assumed that somewhere in the spectrum the luminosity is mostly due to the inactive galaxy. This is an inexact method to subtract the host galaxy,

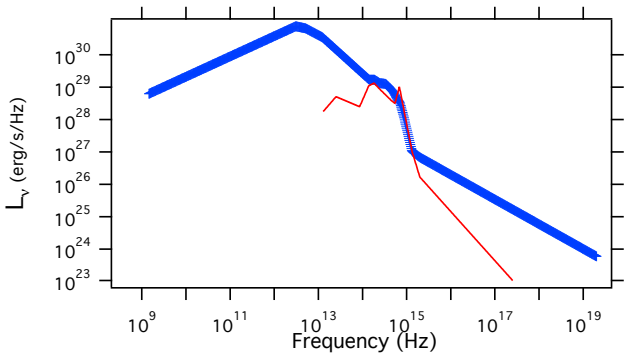

FIG. 9: SED of CGCG 122-055 a galaxy defined as a Seyfert in both BPT diagrams. The blue line represents CGCG 122-055 and the red line represents the scaled SED of NGC 221. The scaling factor is 140.

but it is a good estimate. Fig. 9 is an example of one of these graphs. Just like in Fig. 5 the SED of the AGN is plotted, but this time the host galaxy estimate has been plotted alongside and scaled to the AGN. Once the host galaxy has been scaled the luminosity can be calculated using

$$L_{AGN} = L_{tot} - L_{host}. \tag{13}$$

The Eddington ratio can be calculated now that both the AGN luminosity and the black hole mass, and by chain the Eddington Limit, have been calculated. Table 2 has the data collected for all of the galaxies which were analyzed by means of their SED. Each galaxy is given a galaxy number in the first column in the table, the specific galaxy each of these numbers refers to can be seen at the end of the paper. The last column on the right is the value for the logarithm of the Eddington Ratio as found in Eqn. 9. The difference in values from the two methods of finding the Eddington Ratio is quite apparent with the method utilized in this paper typically giving an Eddington Ratio a factor of 10 higher. The only exception to this is galaxy 8, which actually had a lower Eddington Ratio derived from SED analysis. It is hard to say exactly why this is, but it could be due to the fact that the SED method examined the AGN at all wavelengths and did not assume anything about the broad Hα line. Clearly, looking at the SEDs in Fig. 5 and 9 the AGN lets off a huge amount of light in the far infrared, which is unaccounted for in equation 9. Stern and Laor [2][3] had to use this estimate, however because they wanted to examine large bins and not just single galaxies. On top of this they did not always have data in every part of the spectrum so they had to find a way to get the Eddington ratio based on what they had.

With the newly derived Eddington Ratios the graphs from above could be recreated. Fig. 10 shows the rotated [OI] BPT diagram of the galaxies examined by means of their SED. Each different galaxy can be seen based on the galaxy number from table 2. It can be seen that 9-12, all the galaxies defined as Seyferts in both diagrams, are

TABLE II: Data Derived from SEDs

Galaxy No.	[OI] Class.	[SII] Class.	Log(L/L$_{EDD}$)	L$_{AGN}$ ($\frac{erg}{s}$)	Eqn. 9 Est.
1	LINER	LINER	-0.64	1.43×10^{44}	-2.19
2	LINER	LINER	-1.20	3.67×10^{44}	-2.45
3	LINER	LINER	-1.22	1.22×10^{44}	-1.49
4	LINER	LINER	-1.76	2.466×10^{44}	-2.52
5	LINER	Seyfert	-1.78	7.00×10^{43}	-2.79
6	LINER	Seyfert	-1.53	2.99×10^{44}	-2.55
7	Seyfert	LINER	-1.52	9.24×10^{43}	-2.60
8	Seyfert	LINER	-1.50	3.24×10^{44}	-1.46
9	Seyfert	Seyfert	-2.018	5.74×10^{43}	-3.15
10	Seyfert	Seyfert	-0.738	1.26×10^{44}	-1.38
11	Seyfert	Seyfert	-0.662	2.22×10^{44}	-1.68
12	Seyfert	Seyfert	-0.044	4.36×10^{44}	-1.54

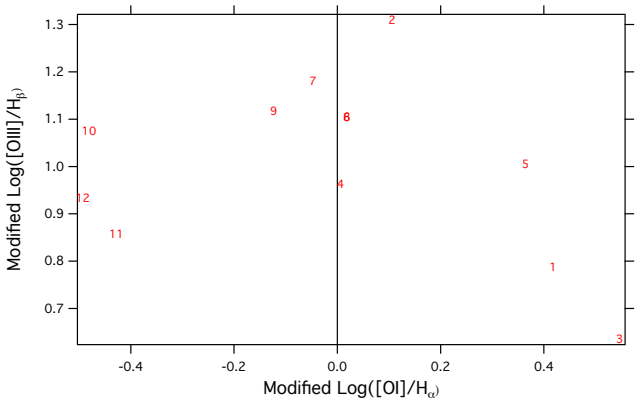

FIG. 10: Rotated [OI] BPT diagram of just the galaxies examined in table 2. The numbers correspond to the numbers in the first column in table 2 as well as marking their location on the plot.

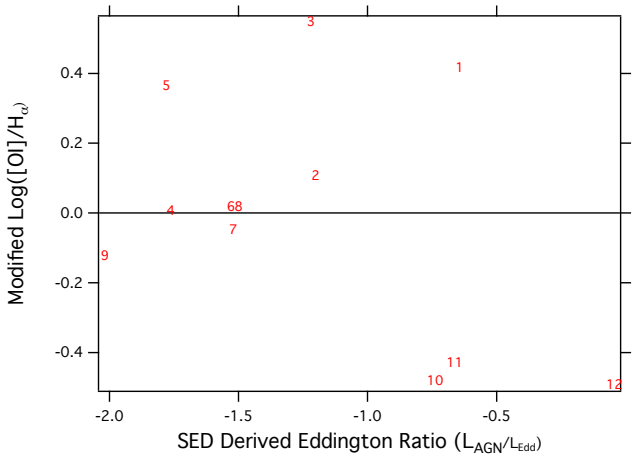

FIG. 11: The Eddington Ratio derived by the SED plotted with the rotated and shifted [OI] ratio. No trend is seen with the galaxies as the LINERs are still spread out in all Eddington Ratio values.

the furthest to the left and the LINERs seem to be a bit more spread out. This is a consequence of the the galaxies chosen. With the rotated axes now the Eddington ratio can be plotted as in Fig. 11 and 12. In both figures no trend can be seen as the LINERs are spread out in all different values of Eddington Ratio.

There was no trend seen in this study, but that does not mean that there is definitively no relationship between the Eddington Luminosity and the placement of a galaxy on a BPT diagram. Only 12 galaxies were studied here and many more need to be analyzed before a concrete conclusion can be reached.

V. CONCLUSION

In this study we wanted to expand on the work of Stern and Laor [2][3] by examining the SEDs of select galaxies in their studies and finding their Eddington Ratios. Using Stern and Laor's data the Eddington Ratio, as

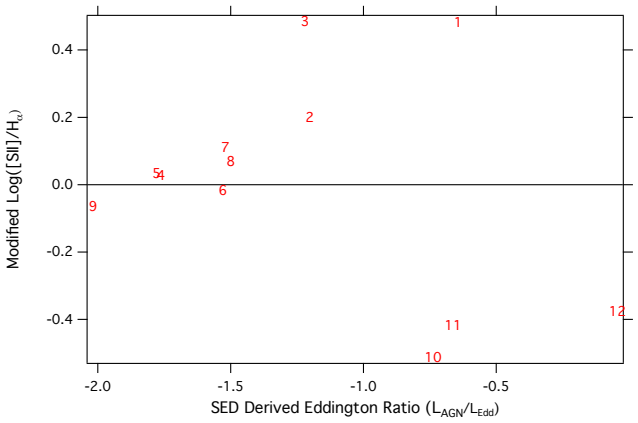

FIG. 12: Modified [SI] ratio plotted against the SED derived Eddington Ratio. Similarly to Fig. 11 a slight trend can be seen with the LINERs moving up and to the right.

TABLE III: Galaxy Numbers Defined

Number	Galaxy
1	NGC 3884
2	NGC 4619
3	2MASX J15485587+5328497
4	2 MASX J11015818+1205311
5	UGC 06614
6	2MASX J16311554+2352577
7	NGC 6418
8	2MASX J00351149-0049184
9	NGC 4235
10	MRK 1310
11	CGCG 122-055
12	UGC 07065

derived by Stern and Laor, was plotted on graph along with the x-axis from the rotated BPT diagram. This lead to a plot that showed no trend between the Eddington Ratio and the placement on the diagram. To see if how they derived the Eddington ratio lead to accurate results SEDs were analyzed from several galaxies. As a whole the Eddington Ratio derived through SED analysis yielded a larger Eddington Ratio then the one derived by Stern and Laor using Eqn. 9. There was also still no trend noticed in the placement of the galaxies in relation to the Seyfert/LINER dividing line. Although this is not definitive as only 12 galaxies were analyzed by their SED. To come to a complete answer to this question a few thousand galaxies must be analyzed by the same method. Therefore for any future work there must be a way to analyze these SEDs in a greater volume and faster as it is unrealistic to analyze thousands of galaxies one at a time.

VI. ACKNOWLEDGMENTS

I would like to thank Dr. Karen Lewis, Dr. Susan Lehman, and the rest of the College of Wooster physics department for making this project possible. This research has made use of the NASA/IPAC Extragalactic Database (NED) which is operated by the Jet Propulsion Laboratory, California Institute of Technology, under contract with the National Aeronautics and Space Adminstration.

[1] B.M. Peterson *An Introduction to Active Galactic Nuclei*, (Cambridge University Press, United Kingdom, 1997), pp. 1-63, 93-106.
[2] Stern, J., Laor, A., MNRAS **423** 600 (2012)
[3] Stern, J., Laor, A., MNRAS **431** 836 (2013)
[4] "Active Galactic Nuclei Example Spectrum", Accessed April 27, 2015, http://archive.stsci.edu/hut/instruments/n4151.html?print=1
[5] "LINERs" Astronomical Glossary, Accessed April 16, 2015, http://ned.ipac.caltech.edu/level5/Glossary/Essay_liner.html
[6] Baldwin, J. A., Phillips, M. M., Terlevich, R. PASP **93**, 5 (1981).
[7] Storm, Allison "Separating AGN activity form star formation at high redshift", Astrobites, Accessed April 17, 2016, http://astrobites.org/2012/12/16/separating-agn-activity-from-star-formation-at-high-redshift/
[8] J Wang et al., 2009 ApJ 693 L66
[9] Kewley, L., Groves, B., Kauffmann, G., Heckman, T., Mon. Not. R. Astron. Soc **372** 961 (2006)
[10] Osterbrock, D.E.,Ferland, G.J. *Astrophysics of Gaseous Nebulae and Active Galactic Nuclei* (University science Books, United States, 2006) pp. 171, 353-390
[11] Greene, J. E., Ho, L.C. ApJ **630** 122 (2005)
[12] Doe, S., Et. Al, Astro. Data. Ana. Softw. and Sys., **461** 893 (2012)
[13] Richards, G. T., et al., Ast Jour Sup Ser, **166** 470 (2006)